ELSEVIER

Biochimica et Biophysica Acta 1562 (2002) 45–56

BIOCHIMICA ET BIOPHYSICA ACTA
BBA

www.bba-direct.com

Secondary structure of spiralin in solution, at the air/water interface, and in interaction with lipid monolayers

Sabine Castano [a,*], Daniel Blaudez [b], Bernard Desbat [a], Jean Dufourcq [c], Henri Wróblewski [d]

[a] *LPCM-CRCM, UMR CNRS 5803, University Bordeaux I, 33405 Talence, France*
[b] *CPMOH, UMR CNRS 5798, University Bordeaux I, 33405 Talence, France*
[c] *CRPP-CNRS, 33600 Pessac, France*
[d] *UMR CNRS 6026, University Rennes I, 35042 Rennes, France*

Received 1 October 2001; received in revised form 31 January 2002; accepted 4 February 2002

Abstract

The surface of spiroplasmas, helically shaped pathogenic bacteria related to the mycoplasmas, is crowded with the membrane-anchored lipoprotein spiralin whose structure and function are unknown. In this work, the secondary structure of spiralin under the form of detergent-free micelles (average Stokes radius, 87.5 Å) in water and at the air/water interface, alone or in interaction with lipid monolayers was analyzed. FT-IR and circular dichroism (CD) spectroscopic data indicate that spiralin in solution contains about 25 ± 3% of helices and 38 ± 2% of β sheets. These measurements are consistent with a consensus predictive analysis of the protein sequence suggesting about 28% of helices, 32% of β sheets and 40% of irregular structure. Brewster angle microscopy (BAM) revealed that, in water, the micelles slowly disaggregate to form a stable and homogeneous layer at the air/water interface, exhibiting a surface pressure up to 10 mN/m. Polarization modulation infrared reflection absorption spectroscopy (PMIRRAS) spectra of interfacial spiralin display a complex amide I band characteristic of a mixture of β sheets and α helices, and an intense amide II band. Spectral simulations indicate a flat orientation for the β sheets and a vertical orientation for the α helices with respect to the interface. The combination of tensiometric and PMIRRAS measurements show that, when spiroplasma lipids are used to form a monolayer at the air/water interface, spiralin is adsorbed under this monolayer and its antiparallel β sheets are mainly parallel to the polar-head layer of the lipids without deep perturbation of the fatty acid chains organization. Based upon these results, we propose a 'carpet model' for spiralin organization at the spiroplasma cell surface. In this model, spiralin molecules anchored into the outer leaflet of the lipid bilayer by their *N*-terminal lipid moiety are composed of two colinear domains (instead of a single globular domain) situated at the lipid/water interface. Owing to the very high amount of spiralin in the membrane, such carpets would cover most if not all the lipids present in the outer leaflet of the bilayer.

Keywords: Spiralin; α Helix; β Sheet; Protein–lipid interaction; Monolayer; FT-IR and PMIRRAS spectroscopy; Brewster angle microscopy

1. Introduction

The spiroplasmas form a group of pathogenic bacteria related to the mycoplasmas [1]. In contrast to the vast majority of eubacteria, their cell envelope being devoid of a cell wall, is composed of only the plasma membrane. The spiroplasma cell is helically shaped under favorable growth conditions and displays a vigorous motility based upon swimming periods alternating with direction changes [2]. Swimming and re-orientations are due to a screw-like rotation and to flexions and contractions of the cell helix, respectively [3,4]. A membrane-bound cytoskeleton which follows, intracellularly, the shortest helical line on the cellular coil seems to play a central role in spiroplasma cell shape and motility [5,6]. The fibrils of this cytoskeleton are composed of a single protein species [7], whose gene (*fib*) has been sequenced [8]. The cell membrane of spiroplasmas is also characterized by the presence of spiralin, a major lipoprotein accounting for up to 20–30% of the total membrane protein mass in these bacteria [9,10]. An *N*-terminal *N*-acyl(*S*-diacylglyceryl) cystein anchors spiralin into the outer leaflet of the membrane lipid bilayer [11–13], while the whole polypeptidic chain is exposed to the outer medium [11]. Interestingly, the *N*-terminus of this lipoprotein is responsible for its immunomodulatory activity [14].

* Corresponding author. Laboratoire de Physico-Chimie Moléculaire, University Bordeaux I, 33405 Talence, France. Tel.: +33-5-5684-6364; fax: +33-5-5684-8402.
E-mail address: castano@morgane.lsmc.u-bordeaux.fr (S. Castano).

0005-2736/02/$ - see front matter
PII: S0005-2736(02)00366-8

To date, neither the structure nor the cell function of spiralin are known, although spiralin genes from several species of spiroplasmas have been sequenced [15,16]. The failure to find a spiralin homolog in data banks suggests that this protein is specific to the spiroplasmas.

Since spiralin accounts for about 25% of the whole membrane protein mass [10] and is a rather small protein (219 amino acid residues in *Spiroplasma melliferum*, [15]), the spiroplasma membrane outer surface is crowded with spiralin molecules. We hence believe that its cellular function is very probably a structural and mechanical one rather than a catalytical one. Since spiroplasmas are obligate parasites of animals or plants, spiralin might protect the lipids and possibly the proteins of the spiroplasma cell membrane against host lipases and proteases. Furthermore, owing to its very high abundance on the cell surface, it probably influences membrane curvature and thus contributes, at least to some extent, in addition to the contractile cytoskeleton, to cell shape determination. It should be noted, however, that the mechanism responsible for the spiroplasma helical shape and motility being coupled to the transmembrane electrical potential of the cell [17–19] is certainly more complex than would suggest just the asymmetric localization of spiralin.

We have addressed the problem of the structure of spiralin and its interfacial properties, by analyzing the secondary structure of the pure molecule in water by infrared (IR) and circular dichroism (CD) spectroscopy. The data thus obtained were compared with structure predictions deduced from the spiralin amino acid sequence. Furthermore, its structure and orientation at the air/water interface in the presence or absence of a lipid monolayer were analyzed by polarization modulation infrared reflection absorption spectroscopy (PMIRRAS). Finally, the lateral distribution of this molecule was observed by Brewster angle microscopy (BAM).

2. Materials and methods

2.1. Chemicals

Dimyristoylphosphatidylcholine (DMPC), dimyristoylphosphatidylglycerol (DMPG), and phosphatidylserine (PS) from Avanti Polar Lipids (Birmingham, AL) were solubilized in chloroform or chloroform/methanol (10%, v/v) at about 5 mM. *N*-lauroyl sarcosine (Sarkosyl) and 3-[(3-cholamidopropyl) dimethylammonio]-1-propyl sulfonate (CHAPS) were obtained from Sigma (USA). Organic solvents, methanol and $CHCl_3$ from Prolabo, were the purest available.

2.2. Spiralin purification

S. melliferum BC3 was grown and plasma membranes were isolated as previously described [20]. Spiralin was purified by preparative agarose suspension electrophoresis in the presence of 10 mM CHAPS after selective extraction with 100 mM CHAPS from the membrane protein fraction insoluble in 10 mM Sarkosyl [9,20]. Detergent-free spiralin micelles were obtained by dialysis against 50 mM sodium phosphate buffer pH 7.4 for 6 days at room temperature. Hydrophobic beads (BioBeads SM-2 from BioRad, USA) were used to adsorb detergent molecules diffusing out of the dialysis bag. The concentration of the protein was finally adjusted to 4 mg/ml.

2.3. Size-exclusion chromatography

Since spiralin molecules assemble in water in the absence of detergent under the form of globular lipoprotein micelles [20], the preparation described above was subjected to size-exclusion chromatography to assess its homogeneity and determine the Stokes radius of the micelles. The chromatographies were performed at room temperature in a Superdex 200 HR column (diameter, 1 cm; height, 30 cm) (Pharmacia, Uppsala, Sweden). The buffer used for column equilibration and protein elution (0.4 ml/min) was 50 mM sodium phosphate buffer pH 7.0 containing 0.15 M NaCl. Spiralin and reference proteins (thyroglobulin, ferritin, catalase, apotransferrin, hemoglobin and cytochrome *c*) were detected by light absorption at 280 nm. A plot of the elution volumes (V_e) vs. log Stokes radii (R_s) of spiralin and of the reference proteins was used for the determination of spiralin micelles R_s.

2.4. Spiroplasma membrane lipid extraction

Pellets of isolated *S. melliferum* membranes were extracted three times for 30 min at room temperature and in the dark with 20 volumes of chloroform–methanol (2:1, v/v). After each extraction, proteins were removed by centrifugation ($3000 \times g$, 15 min, 18 °C). The clear lipid solutions were pooled, dried under a stream of nitrogen and stored at −80 °C. The lipids were solubilized in chloroform (10 mg/ml) just before use.

2.5. Protein and cholesterol determination

Spiralin concentration was determined by the bicinchoninic acid method using acetone-washed and dried spiralin as standard [21]. Total cholesterol was colorimetrically determined in the spiroplasma purified lipid fraction using the Sigma Diagnostics cholesterol reagent kit (Sigma, St. Louis, MO).

2.6. Secondary structure prediction

Secondary structure prediction of spiralin was performed by analyzing the amino acid sequence with a combination of the following methods: HNN, GOR IV, SIMPA96, SOPMA and PHD via NPS@, the Network Protein Sequence Analysis [22].

2.7. Circular dichroism spectroscopy

Circular dichroism of spiralin detergent-free micelles was recorded between 190 and 250 nm at 20 °C with a Jobin–Yvon Mark V dichrograph equipped with a thermostatically controlled quartz cell with a path length of 1 mm. The sample contained 0.4 mg of protein per ml of 10 mM sodium phosphate buffer pH 7.4. For each analysis, at least three scans were performed and subsequently averaged. Corrections were made for buffer contribution. The singular value decomposition (SVD) method was used for the deconvolution of the spectra [23].

2.8. Film formation and surface pressure measurements

The experiments were performed on a homemade glass rectangular Langmuir trough (18 cm^3, 50 cm^2), since spiralin displayed a very high affinity for the walls of the 'classical' teflon troughs. The surface pressure (Π) was measured by the Wilhelmy method using a filter paper plate. The trough was filled with 60 mM phosphate buffer pH 7.3, using ultra pure water (Milli-Q, Millipore). The experiments were carried out at 23 ± 2 °C. A few microliters of spiralin stock solution (4 mg/ml in phosphate buffer 25 mM, pH 7.4) were always injected into the subphase to define the total spiralin concentration.

To obtain mixed spiralin/lipid films, lipids were spread at the air/water interface from chloroform or chloroform/methanol (10%, v/v) solutions using a Hamilton microsyringe until the desired pressure was reached. In a second step, a few microliters of the spiralin stock solution were injected into the subphase and the pressure increase ($\Delta\Pi$) was recorded for each spiralin concentration after 30–40 min.

2.9. FT-IR and PMIRRAS spectroscopy measurements and spectral simulations

The absorbance spectrum of a bulk sample of spiralin was obtained by conventional FT-IR transmission spectroscopy after the aqueous solution was evaporated on a ZnSe window while the absorbance spectra of spiralin micelles in water was done in a CaF_2 liquid cell with modulable thickness.

Interface studies of spiralin and mixed spiralin/lipid monolayers were done in situ by PMIRRAS. The spectra were recorded on a Nicolet 740 spectrometer equipped with a HgCdTe detector cooled at 77 K. Generally, 200 or 300 scans were coadded at a resolution of 4 and 8 cm^{-1} for pure spiralin or mixed spiralin/lipid monolayers, respectively. Briefly, PMIRRAS combines FT-IR reflection spectroscopy with fast polarization modulation of the incident beam between parallel (p) and perpendicular (s) polarizations [24–27]. Two-channel processing of the detected signal allows to obtain the differential reflectivity spectrum:

$$\Delta R/R = (R_p - R_s)J_2/(R_p + R_s).$$

To remove the contribution of liquid water absorption and the dependence on Bessel functions, J_2, the monolayer spectrum is divided by that of the subphase. When the incidence angle is fixed at 75°, transition moments preferentially oriented in the plane of the interface give intense and upward-oriented bands, while perpendicular ones give weaker and downward-oriented bands.

The decomposition of the amide I spectral region (1600–1800 cm^{-1}) into individual bands was performed with the Peaksolve (version 3.0, Galactic) software and analyzed as a sum of Gaussian/Lorentzian curves, with consecutive optimization of amplitudes, band positions, half-widths and Gaussian/Lorentzian compositions of the individual bands.

PMIRRAS spectra of protein monolayer at the air/water interface were calculated with a homemade software based on the 4×4 matrix formalism of Berreman [28,29]. The infrared optical indices of the isotropic and oriented protein structures have been calculated using the optical indices of the pure secondary structures (α helices, β sheets) previously determined [30].

2.10. BAM measurements

The morphology of pure spiralin and mixed spiralin/lipid layers at the air/water interface were observed using a Brewster angle microscope (NFT BAM*2plus*, Göttingen, Germany) mounted on the glass Langmuir trough. The microscope was equipped with a frequency doubled Nd:Yag laser (532 nm, 20 mW), polarizer, analyser and a CCD camera. The spatial resolution of the BAM was about 2 μm and the image size 625×500 μm.

3. Results

3.1. Spiralin micelles size

An average Stokes radius of 87.5 ± 7.5 Å was determined for spiralin micelles by size-exclusion HPLC in the complete absence of detergent. Since the aggregates are spherical [14], an average diameter of 175 Å corresponds to the size of a globular protein of ca. 700 kDa, equivalent to about 28 monomers of spiralin. Assuming the core of the micelles is filled with the fatty acyl chains (three per monomer), while the crust is composed of the polypeptide chains, such a ratio cannot be obtained with compact monomers having a diameter of 38 Å (i.e. the diameter of a spiralin polypeptide chain if it were globular and extremely compact). The structure of the micelles can thus be interpreted as globular aggregates of lipoprotein monomers whose polypeptide chain displays a more elongated and probably flexible structure.

3.2. Prediction of spiralin secondary structure

The amino acid sequence of *S. melliferum* spiralin deduced from the sequence of its gene and after deletion

of the signal sequence upstream of the Cys residue [11] was analyzed using a combination of five different algorithms. The resulting consensus prediction suggests that the secondary structure of spiralin is composed of 28.3% of α helices, 31.5% of β sheets and 40.2% of irregular structure (Fig. 1). According to this approach, spiralin should contain three helices encompassing the sequences P32–K64, K140–I163, and Y183–E188, and nine β strands ranging from 4 to 14 residues and scattered over the whole sequence. It is noteworthy that the second helix has been characterized experimentally by the synthetic peptide approach [11,31] and that, according to the prediction, the first helix might be broken at the level of T54.

3.3. Secondary structures of spiralin in solution

To get a first insight into spiralin secondary structure, the IR spectrum of the lyophilized molecule was registered (not shown). The amide I and II domains, characteristic of the protein, are very broad and centered around 1650 and 1545 cm^{-1}, respectively. The broad amide I domain shows a very complex structuration and the contribution of numerous secondary structures: α helices, β sheets, β turns and coils.

In aqueous solution, i.e. in conditions more relevant to the native state, spiralin displayed a high tendency to self-aggregate into globular micelles (see Spiralin micelles size). The IR spectrum in solution was hence characteristic of self-

```
 1                                                  25
C N K T E S N N L S R V K T I A A P A T V A A S T
c c c c c c c c c c c e e e e e c c c c c c c c c

 26                                                 50
P K A V T K P E I K T A L E A N V L K A V Q G V V
c c c c c c h h h h h h h h h h h h h h h h h h h

 51                                                 75
K T A T A A D F Q F E V Y K N S K G T A L E T I D
h h h c h h h h h h h h h h c c c c c c e e e e e e

 76                                                100
L E A G K V E V Y L Q I T P A K D K T V V I G E T
c c c c c e e e e e e e c c c c c c c e e e e e c c

 101                                               125
R Y I K V T L P K H G E V T K V D I K D V T V T E
e e e e e e e c c c c e e e e e e e e e e e e e e e

 126                                               150
Q T V G I K A S T P K A V K K D E L N A V N T Y A
e e e e e e c c c c c c c c c h h h h h h h h h h h

 151                                               175
T L A K A V L D A I Q N I A P N A G A S D F E I T
h h h h h h h h h h h h h c c c c c c c c c e e e e

 176                                               200
N N G A E G D Y E A A K E V E V T V K A K N D S A
c c c c c c c c h h h h h h e e e e e e e c c c c c c

 201                                 219
N I S G Q F K F K A K V T A T A P T E
c c c c e e e e e e e e e c c c c c c
```

Fig. 1. Spiralin sequence and secondary structure predictions by statistical methods. h: α helix; e: β sheet; c: irregular structure (coils and turns).

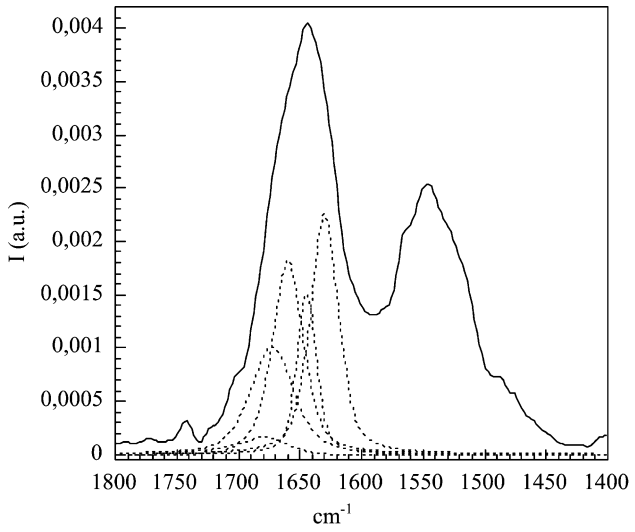

Fig. 2. IR spectrum of spiralin micelles in buffer. (—) Experimental spectrum – [spiralin] = 0.15 mM; (. . .) peaks of the deconvoluted amide I band; phosphate buffer 60 mM, pH = 7.3; T = 23 °C.

aggregated spiralin. It displayed a broad amide I domain centered around 1650 cm^{-1} and an amide II domain around 1550 cm^{-1} (Fig. 2). The deconvolution of the amide I band (Table 1) allowed to attribute the main contributions [32–36] to antiparallel β sheet structures (36 ± 5% with components at 1630 and 1680 cm^{-1}) and α helices (28 ± 5% at 1659 cm^{-1}). β turns (1670 cm^{-1}) and coils (1650 cm^{-1}) represent 22 ± 5% and 14 ± 5% of the secondary structures, respectively.

Independent measurements by circular dichroism (CD) in comparable experimental conditions allowed to attribute 22% of α helices and 40% of β sheets, which is in the range of the data obtained by FT-IR (Table 1). Overall contributions of β turns and coils are estimated to be 38% due to the inability of the CD technique to accurately detect these types of secondary structures.

3.4. Spiralin adsorption at the air/water interface

Since spiralin displays a very high affinity for teflon and a much weaker tendency to adsorb on glass, the studies of spiralin at the air/water interface were performed in home-made glass Langmuir troughs instead of the usual teflon troughs.

Table 1
Secondary structures of self-aggregated spiralin in aqueous buffer determined by IR and CD spectroscopy

Secondary structure	IR data		CD data
	Amide I frequency (cm^{-1})	Estimated content (%)	Estimated content (%)
antiparallel β-sheet	1630 – 1680	36 ± 5	40 ± 5
α-helix	1659	28 ± 5	22 ± 5
β-turn	1672	22 ± 5	38 ± 5
coils	1644	14 ± 5	

Immediately after spiralin injection into the aqueous subphase, there was a jump in lateral pressure (Π) followed by a progressive and slow increase of Π (7 mN/m in more than 2 h, Fig. 3) demonstrating that spiralin progressively adsorbed at the interface and displayed surface-active properties. At the protein concentrations used, the maximal lateral pressure of 10 mN/m was reached in more than 5 h and the layer formed was stable (not shown).

3.5. Morphology of the spiralin layer at the air/water interface investigated by BAM

BAM images, registered at several lateral pressures during the adsorption kinetics at the air/water interface, displayed a progressive increase of the average normalized gray level from 78 to 231 when lateral pressure increased from 0.5 to 6.5 mN/m (Fig. 4). This progressive variation of luminosity is characteristic both of average thickness and refractive index increases at the interface consecutive to spiralin adsorption. The global homogeneity of the luminosity at the resolution scale of the microscope (2 μm) suggests the homogeneity of the protein layer, which was progressively formed at the interface. The circular domains of more intense luminosity which appeared punctually (Fig. 4, image d) probably correspond to multilayer protein aggregates of higher thickness.

3.6. Structure and orientation of spiralin at the air/water interface investigated by PMMIRAS spectroscopy

Since spiralin formed stable layers at the air/water interface, its structure and orientation in the film were studied, in these conditions, by PMIRRAS spectroscopy. The PMIR-

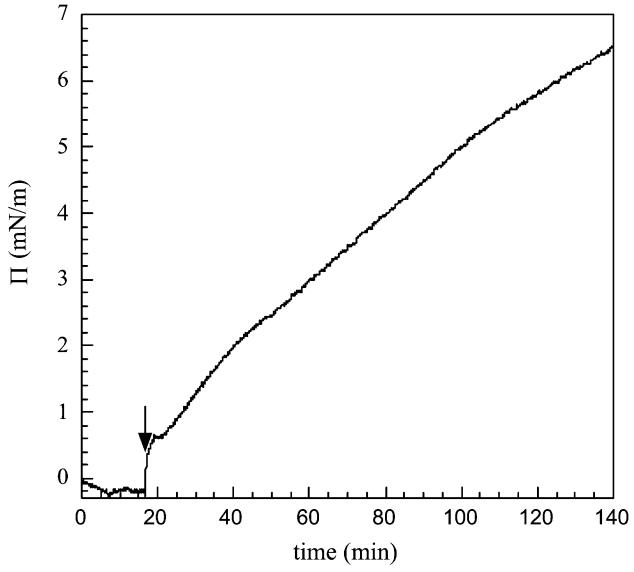

Fig. 3. Kinetics of lateral pressure (Π) increase after spiralin injection (↓) in subphase. [spiralin] = 300 nM. Subphase: phosphate buffer 60 mM, pH = 7.3; T = 23 °C.

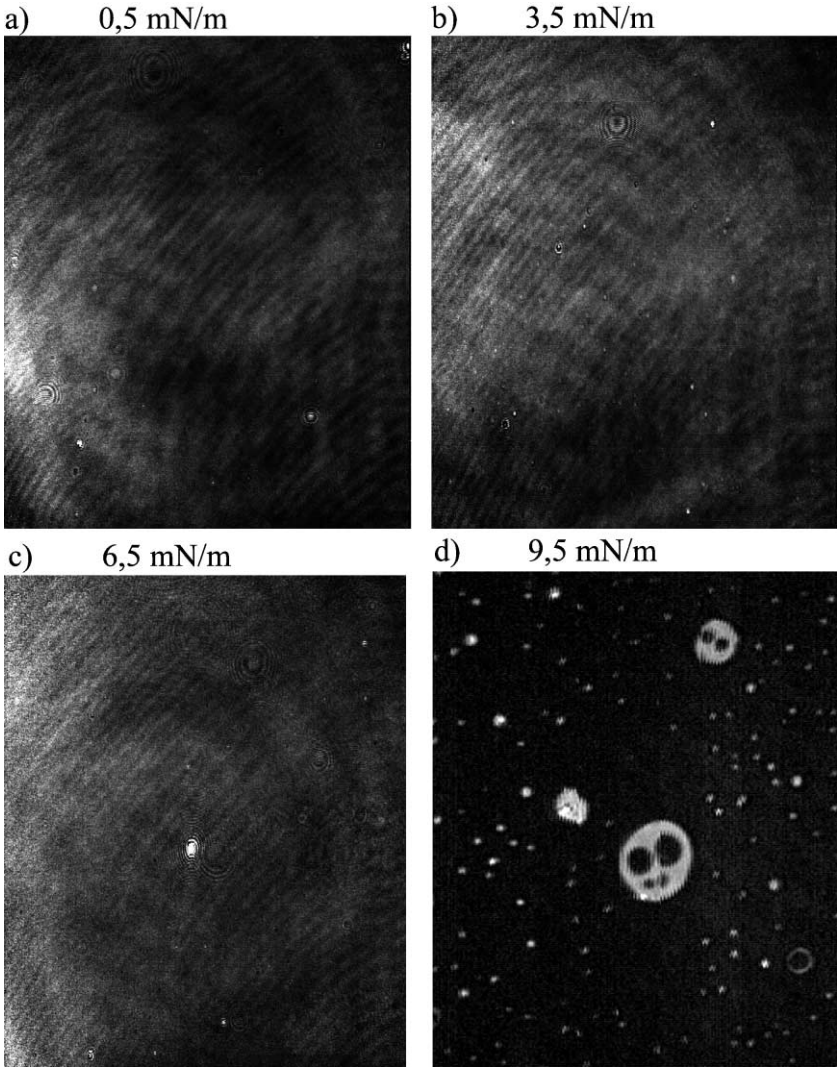

Fig. 4. BAM images of the air/water interface after spiralin injection in the subphase. (a) $\Pi = 0.5$ mN/m–GL = 178–OS = 50. (b) $\Pi = 3.5$ mN/m–GL = 190–OS = 50. (c) $\Pi = 6.5$ mN/m–GL = 96–OS = 120. (d) $\Pi = 9.5$ mN/m–GL = 120–OS = 120. Subphase: phosphate buffer 60 mM, pH = 7.3; $T = 23$ °C. Image size: 625 × 500 μm. Reference black level = 25–GL = gray level; OS = obturation speed.

RAS spectra (Fig. 5) were registered at several lateral pressures after successive protein injections in the subphase.

All the spectra displayed an amide I domain from 1600 to 1700 cm^{-1} and an amide II domain centered around 1540 cm^{-1}. The amide I band contained several contributions with the positive and intense one at 1625 cm^{-1} being characteristic of antiparallel β sheets [32–36]. When the lateral pressure increased, there was an intensification of these two bands showing the progressive increase of spiralin concentration in the IR beam without orientation change. As already described and discussed in previous works [30,37], the additional negative band around 1670 cm^{-1} is characteristic of α helices with peculiar orientation.

To go further in the investigation of the orientation of the identified secondary structures, spectral simulations were performed. Fig. 6 shows the simulated spectra obtained for a layer of spiralin either with an isotropic orientation of the two main secondary structures identified or an anisotropic orientation of the two motifs: a vertical orientation of the α helices and a flat orientation of the β sheets. A good agreement was obtained between the second simulated spectrum and the experimental one in spite of the imprecision on the spiralin indices used for the simulations.

3.7. Spiralin interaction with lipid monolayers

Since spiralin is a protein anchored in the spiroplasma membrane outer leaflet, it was relevant to study its interaction with lipid surfaces. Monolayers of various lipid composition were thus formed at the air/water interface: a monolayer of zwitterionic phospholipids (DMPC), monolayers of negatively charged phospholipids either with saturated and defined chain length (DMPG) or with variable chain lengths and unsaturation (natural PS), and finally with

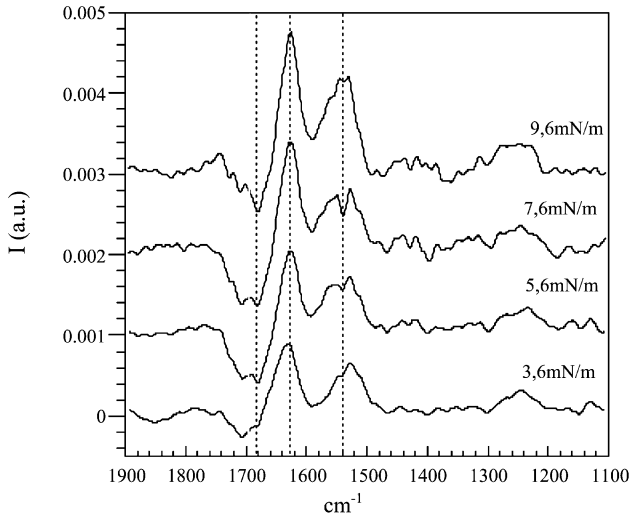

Fig. 5. PMIRRAS spectra of spiralin at the air/water interface. From bottom to top: $\Pi = 3.6$; $\Pi = 5.6$; $\Pi = 7.6$; $\Pi = 9.6$ mN/m. Subphase: phosphate buffer 60 mM, pH = 7.3; $T = 23$ °C.

lipids extracted from spiroplasma membrane (SmBC3 lipids). This latter fraction is a complex mixture of cholesterol, glycolipids and polar lipids [38].

The kinetics of lateral pressure variation ($\Delta\Pi$) of the initially compressed lipid monolayers (15–21 mNm) after spiralin injections in the aqueous subphase are presented in Fig. 7. The $\Delta\Pi$ variations differed significantly according to the lipid composition of the monolayer. The highest $\Delta\Pi$ variations (> 2 mN/m) were obtained for negatively charged phospholipids (DMPG and natural PS). At the same concentration of spiralin in the subphase and during the same time scale, the $\Delta\Pi$ variation observed with zwitterionic

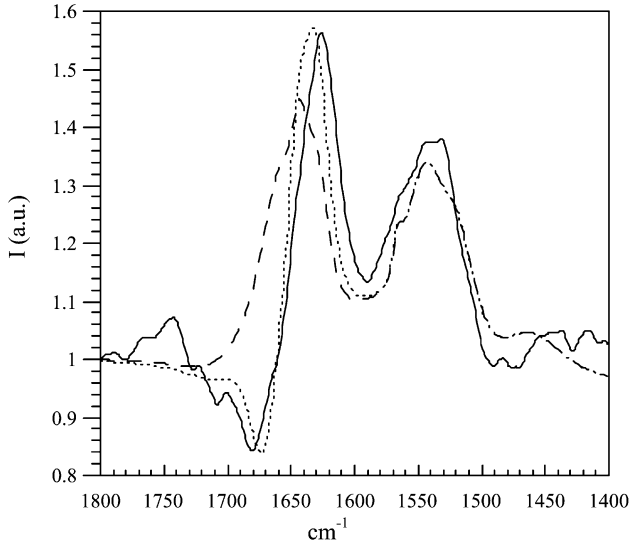

Fig. 6. Simulations of PMIRRAS spectra of spiralin at the air/water interface. (—) PMIRRAS experimental spectrum of spiralin $\Pi = 9.6$ mN/m; (- - -) simulation for an isotropic monolayer of spiralin (10 Å); (. . .) simulation for an anisotropic monolayer of spiralin (10 Å) with flat β sheets and vertical α helices.

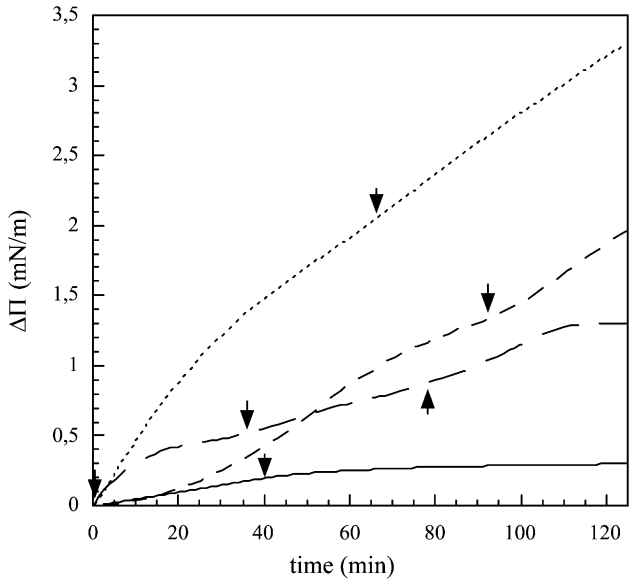

Fig. 7. Kinetics of spiralin interactions with lipid monolayers: variations of lateral pressure of the lipid monolayer ($\Delta\Pi$) after spiralin injections in the subphase. $t = 0$ min: [spiralin] = 83 nM in the subphase. Each arrow (↓) represents an addition of 83 nM of spiralin in the subphase. (- - -) DMPG–$\Pi_0 = 17$ mN/m; (– – –) PS–$\Pi_0 = 21$ mN/m; (— — —) DMPC–$\Pi_0 = 15$ mN/m; (———) spiroplasma lipids (SmBC3)–$\Pi_0 = 16$ mN/m; subphase: phosphate buffer 60 mM, pH = 7.3; $T = 23$ °C.

DMPC was weaker (≈ 0.5 mN/m), while there was almost no $\Delta\Pi$ variation after spiralin injection under the SmBC3 lipid monolayer. It was then possible to establish a hierarchy of spiralin *insertion* into the lipid monolayer as a function of its composition: negatively charged phospholipids (DMPG, natural PS)>zwitterionic phospholipid (DMPC)>natural SmBC3 lipids. It should be noted that although the lack of $\Delta\Pi$ variation characterizes a lack of insertion, it does not rule out the potentiality of protein *adsorption* under the monolayer.

3.8. Structure and orientation of spiralin in mixed protein/lipid layers investigated by PMIRRAS spectroscopy

The in situ PMIRRAS spectra of pure lipid (DMPG, natural PS and SmBC3 lipids) and mixed spiralin/lipid monolayers are presented in Fig. 8. In the spectra of pure lipid monolayers, the bands around 1730 and 1225 cm^{-1} are characteristic of the stretching mode of the C=O ester and phosphate groups of the lipid polar heads, and the band around 1460 cm^{-1} is assigned to the scissoring mode of the methylenes (δ CH_2) of the lipid acyl chains.

The 'subtracted' spectra result from the subtraction of the pure lipid spectrum from the mixed spiralin/lipid one and they allow to extract the characteristic contributions of the protein. A first observation shows that the spiralin spectrum differed strongly according to the lipid monolayer environment. With negatively charged DMPG, the spectrum displays a broad amide I domain. The large and positive component centered around 1653 cm^{-1} is assigned to α

helices mixed with coils. The lack or very weak amide II band reveals an orientation of the helix with its axis parallel to the interface. Deconvolution of this broad amide I domain also allows to assign two positive amide I contributions around 1623 and 1690 cm^{-1}, which are characteristic of β sheets mainly oriented with the strand axis parallel to the interface. The spectrum of spiralin in the negatively charged PS lipids is very different. The amide I domain contains a

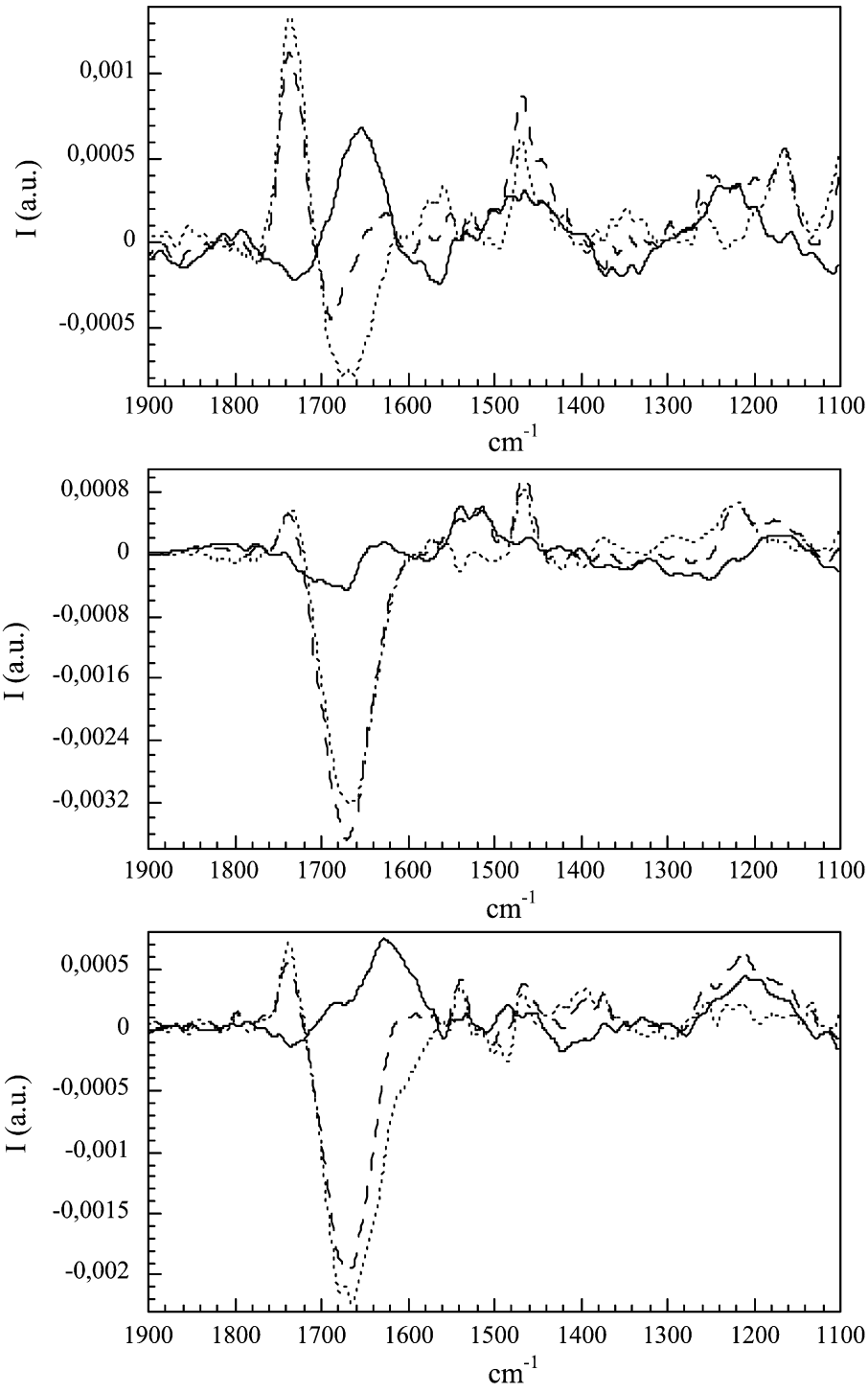

Fig. 8. PMIRRAS spectra of spiralin in interaction with lipid monolayers. Top: (. . .) DMPG monolayer – Π = 17 mN/m; (- - -) mixed spiralin/DMPG monolayer – Π = 22 mN/m; (—) subtracted spectrum – [spiralin] = 166 nM in the subphase. Middle: (. . .) PS monolayer – Π = 21 mN/m; (- - -) mixed spiralin/PS monolayer – Π = 27 mN/m; (—) subtracted spectrum – [spiralin] = 350 nM in the subphase. Bottom: (. . .) spiroplasma lipid (SmBC3) monolayer – Π = 16 mN/m; (- - -) mixed spiralin/SmBC3 lipid monolayer – Π = 16 mN/m; (—) subtracted spectrum – [spiralin] = 166 nM in the subphase. Subphase: phosphate buffer 60 mM, pH = 7.3; T = 23 °C.

positive contribution around 1635 cm^{-1} and a negative one around 1670 cm^{-1}, while the amide II band around 1550 cm^{-1} is rather intense. These features are characteristic of both tilted β sheets and α helices [26,27,37].

Since the structure and the orientation of spiralin were strongly dependent on the lipid environment, the study on natural SmBC3 lipids is more representative of the natural conditions. The PMIRRAS subtracted spectrum of spiralin in the presence of a SmBC3 lipid monolayer displays an intense amide I band characteristic of the protein. Since PMIRRAS spectroscopy is only sensitive to surface contribution, this proves the interaction of spiralin with SmBC3 lipids even if no lateral pressure variation was observed. The amide I domain displays two main positive contributions around 1625 and 1685 cm^{-1} characteristic of antiparallel β sheets mainly oriented parallel to the interface. The band around 1200 cm^{-1} is characteristic of a perturbation of the lipid polar head phosphate groups. The signal to noise ratio on the PMIRRAS spectra does not allow to extract precise information on the lipid chain organization since the $\delta(CH_2)$ band is weak and not very sensitive to disorder. Additionally, all bands involving CH_2 groups also contain the spiralin/lipid chain contribution and cannot be used to draw conclusions about the phospholipid chains modification.

3.9. Morphology of the mixed spiralin/SmBC3 lipid layer at the air/water interface investigated by Brewster angle microscopy

Fig. 9a shows the BAM image of a pure SmBC3 lipid monolayer at 22 mN/m. The image displays a heterogeneous surface with contrasted domains of very high luminosity (normalized gray level 250) in a dark background (gray level 50). This characterizes a phase separation of the

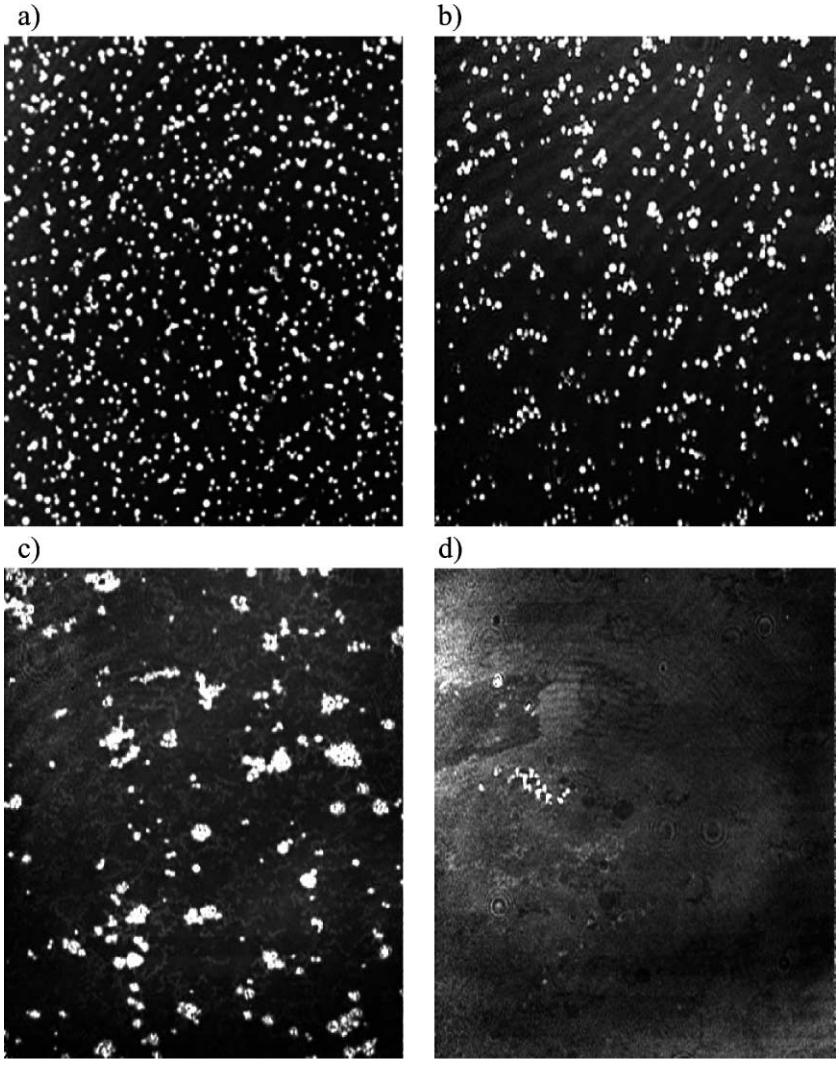

Fig. 9. BAM images of a monolayer of SmBC3 spiroplasma lipid the air/water interface after spiralin injection in the subphase. Spiroplasma lipid monolayer: Image (a) $\Pi = 22$ mN/m–GL = 80–OS = 120. Mixed spiralin/spiroplasma lipid monolayer: Image (b) $\Pi = 22$ mN/m–GL = 80–OS = 120: Image (c) $\Pi = 22$ mN/m–GL = 88–OS = 250: Image (d) $\Pi = 23$ mN/m–GL = 136–OS = 250. Image size: 625 × 500 μm. Reference black level = 25 at OS = 50; [spiralin] = 209 nM in the subphase. Subphase: phosphate buffer 60 mM, pH = 7.3; $T = 23$ °C.

lipids with liquid condensed domains in a liquid expanded phase. When spiralin was injected into the subphase, a change in the morphology of the monolayer was observed (Fig. 9b,c,d). The average normalized gray level, and thus the luminosity, progressively increased from 192 up to 680; these values will be used in the next part to calculate the thickness of the layer at the interface. The initial lipid domains progressively disappeared upon spiralin adsorption and the final state displayed a relatively homogenous phase of very high luminosity.

4. Discussion and conclusion

Secondary structure prediction from the sequence using statistical methods suggests that spiralin is a "mixed" α/β protein containing about 28% of helices, 32% of β sheets and 40% of irregular structures (turns and coils). Direct IR spectrum of lyophilized spiralin, even if these experimental conditions are not relevant for the native structure of the protein in hydrated conditions, confirms the complex folding of the protein. It should be also noted that the predicted amphipathic α helix centered on the A153 residue (Fig. 1) has been experimentally confirmed [11,31] as well as the predicted turn P108–G111. The latter was confirmed by the trypsic cleavage occurring between K109 and H110 [14]. The trypsic dissection of spiralin thus led to the hypothesis that spiralin comprises two distinct domains of comparable size: a trypsin-sensitive domain from C1 to K109 followed by a trypsin-resistant domain from H110 to E219. The first domain displays a very hydrophobic *N*-terminus which, owing to the triacylation of the initial cystein, is responsible for the amphiphilicity of spiralin. However, the absence of any predicted membrane spanning hydrophobic helix within the sequence of spiralin [11] indicates that both domains are exposed on the surface of the spiroplasma cell.

To go further, it was more relevant to study spiralin structure in aqueous conditions, since protein structure is strongly dependent on hydration [39,40]. Since spiralin strongly self-aggregates in solution and forms globular micelles of 175 ± 15 Å diameter, the IR and CD spectra recorded for aqueous solutions of spiralin are characteristic of secondary structure of spiralin in detergent-free lipoprotein micelles. There is a relatively good agreement between the results obtained by these two independent methods since both identify a main contribution of β sheets ($38 \pm 2\%$), while α helices represent $25 \pm 3\%$ of the secondary structure. Furthermore, there is also a good agreement between the structural predictions and the spectroscopic data for spiralin in solution.

Spiralin forms stable layers at the air/water interface and displays surface-active properties. Thus, its tertiary folding exhibits an amphipathic character with the polypeptide probably in contact with water and the *N*-terminus with the three acyl chains in the air. The progressive kinetics of spiralin adsorption at the air/water interface reflects the slow disaggregation process of the stable spiralin micelles in solution. The homogeneous and progressive increase of luminosity observed on the BAM images obtained during spiralin adsorption characterizes the increase of the protein concentration at the interface to form a homogeneous phase at the resolution scale of the microscope (2 μm). Using a spiralin refractive index of $n = 1.53$ [41], the software incorporated in the BAM microscope gives an average thickness of 15 Å for the more condensed protein layer. The diameter of a spiralin polypeptide folded under a single compact and globular domain would be of 38 Å. Thus, even if the calculation performed using the BAM images is only an estimation, it strongly suggests that a monolayer of spiralin forms at the interface and the protein does not adopt a globular form but a more extended and flat organization. This hypothesis is consistent with the diameter of the spiralin micelles obtained in detergent-free solutions and is confirmed by the PMIRRAS spectra which display a complex amide I band and an intense amide II band, characteristic of a mixture of β sheets and α helices. Spectral simulations show that β sheets adopt a flat orientation at the interface. The accumulation of spiralin molecules at the interface leads to both an increase of the lateral pressure and of the amide β sheet band intensity. Additionally, the negative band around 1670 cm^{-1} shows the progressive tilt of the α helices towards a more vertical orientation when Π increases. This structuration and anisotropic flat orientation of the β sheets parallel to the interface plane are in good agreement with the weak thickness value estimated by BAM. Thus, even if PMIRRAS spectroscopy does not solve the tertiary structure of spiralin, i.e. the 3-D arrangement of the identified secondary structures, it allows to conclude to a peculiar organization and orientation of the different structural motifs.

Since spiralin is a membrane-anchored lipoprotein, its study in interaction with lipid monolayers stabilized at the air/water interface presents a great interest to better understand its properties and those of similar molecules. The measured lateral pressure variations show that the mechanism of interaction, the structure and the orientation of the protein are strongly dependent on the nature of the lipid environment. The $\Delta\Pi$ increase indicates that spiralin inserts in negatively charged phospholipid monolayers of DMPG and PS. In contrast, on natural SmBC3 lipid monolayers, the lack of or very weak $\Delta\Pi$ increase, together with the amide I band characteristic of spiralin on PMIRRAS spectrum indicate that spiralin adsorbs mainly under this lipid monolayer. Actually, the PMIRRAS spectra show a versatile folding of spiralin depending on the lipid environment. A mixed antiparallel β sheet/α helical structure was observed on the negatively charged DMPG and PS phospholipids, but while the main axis of both structures was parallel to the interface in the case of DMPG, a tilted orientation was observed when spiralin inserted into PS lipids. On spiroplasma lipids, the PMIRRAS spectrum allows to conclude that spiralin mainly folds into antiparallel β sheets with a

flat orientation of the strands at the interface. The relative width of the amide I band shows the presence of other secondary structures, which are mainly flat-oriented at the interface since the amide II band is very weak. Furthermore, on the subtracted spectrum, the band around 1200 cm^{-1} is characteristic of a perturbation of the lipid polar head phosphate groups proving the adsorption of spiralin under the monolayer without deep perturbation of the lipid molecular organization. These results are then consistent with a 'carpet model' of spiralin molecules anchored in the lipid monolayer by their own acyl chains, and inducing neither severe changes in the lipid chains organization nor important $\Delta\Pi$ increases. In this model, the protein is flat-adsorbed under the lipid monolayer, occupying a large molecular area and only perturbing the lipid polar heads.

Thus, independent of the lipid environment, spiralin structure and orientation are different from those observed for pure spiralin at the air/water interface. It is also important to emphasize that due to the versatility of the protein structure, the study on spiroplasma lipids are the most relevant with respect to the natural in vivo conditions. Therefore, only the morphology of mixed spiralin/spiroplasma lipid monolayer was further investigated by BAM. The image of the pure (protein-free) spiroplasma lipid monolayer compressed to 22 mN/m is characteristic of a biphasic mixture of liquid condensed domains in a liquid expanded fluid phase. From the average gray level, it is possible to estimate the thickness of the lipid monolayer using $n=1.50$ for the lipid refractive index [42]. The estimation gives a thickness of 17 Å, in good agreement with the thickness expected for the half of a membrane. The progressive spiralin adsorption led to an important increase of luminosity and a higher homogeneity of the surface layer. Several concomitant phenomena can explain these observations. The homogeneous spiralin adsorption under the lipid monolayer leads to changes both in layer refractive index and thickness, and contributes to the homogeneous increase of luminosity. Simultaneously, changes in the morphology of the lipid monolayer can happen to lead to a more homogeneous liquid expanded or condensed phase. Even if it is not possible to accurately deconvolute the respective contributions of the two phenomena, the lack of important perturbation in lipid organization observed by PMIRRAS spectroscopy favors the first one. Again, the relatively homogeneous gray level at the final state allows to estimate the average thickness of the mixed spiralin/spiroplasma lipid layer, using a homemade software [43] to model the two layers with refractive indexes of $n=1.50$ and $n=1.53$ for the lipids and the protein, respectively. A total thickness of 25–30 Å was estimated. This gives an 8–13-Å thickness for the adsorbed protein layer taking into account the 17-Å thickness of the lipid layer and hypothesizing that there is no significant change in the lipid layer due to spiralin adsorption. Such a calculation suggests again that only a monolayer of spiralin is adsorbed under the lipid layer. The weak thickness compared to the 38 Å of a single-domain, globular protein is also in good agreement with the anisotropic and flat orientation of the protein antiparallel β sheets at the lipid interface.

Altogether these results are consistent with 'spiralin carpets' anchored in the outer leaflet of the membrane by their lipid moiety but without penetration of the polypeptide chain within the bilayer. The weak 8–13 Å thickness of the spiralin adsorbed layer and the main antiparallel β sheet folding with a flat orientation at the interface rules out the hypothesis of a compact and globular protein since this one would give a much larger thickness (38 Å). Furthermore, these results support the hypothesis that spiralin is composed of two colinear domains, both adsorbed on the lipid polar heads, the first one being tightly anchored to the membrane by the acyl chains of the N-terminus. Owing to the very high amount of spiralin in the membrane (25–30% of the total membrane protein mass [9,10]), such carpets should cover most if not all the lipids present in the outer leaflet of the bilayer suggesting a dual role of spiralin protecting the lipids of the membrane outer layer and, at the same time, influencing membrane curvature. Since *S. melliferum* is a honey bee pathogen devoid of a cell wall [44], the protection of its membrane lipids by spiralin (e.g. against lipases) might be crucial for its survival in the digestive tract of the insect. Further investigations are necessary to solve precisely the tertiary structure of the protein and the relative orientation of the two protein domains.

Acknowledgements

This work was partly supported by the ''Programme Physique et Chimie du Vivant'' (CNRS).

References

[1] S. Razin, D. Yogev, Y. Naot, Microbiol. Mol. Biol. Rev. 62 (1998) 1094–1156.
[2] R.M. Cole, J.G. Tully, T.J. Popkin, J.M. Bové, J. Bacteriol. 115 (1973) 367–386.
[3] M.J. Daniels, J.M. Longland, Curr. Microbiol. 10 (1984) 191–194.
[4] M.J. Daniels, J.M. Longland, J. Gilbart, J. Gen. Microbiol. 118 (1980) 429–436.
[5] D.L. Charbonneau, W.C. Ghiorse, Curr. Microbiol. 10 (1984) 65–72.
[6] S. Trachtenberg, R. Gilag, Mol. Microbiol. 41 (2001) 827–848.
[7] R. Townsend, D.B. Archer, K.A. Plaskitt, J. Bacteriol. 142 (1980) 694–700.
[8] D.L. Williamson, J. Renaudin, J.M. Bové, J. Bacteriol. 173 (1991) 4353–4362.
[9] H. Wróblewski, K.E. Johansson, S. Hjertén, Biochim. Biophys. Acta 465 (1977) 275–289.
[10] H. Wróblewski, D. Robic, D. Thomas, A. Blanchard, Ann. Microbiol. (Ann. Inst. Pasteur) 135A (1984) 73–82.
[11] C. Brenner, H. Duclohier, V. Krchnák, H. Wróblewski, Biochim. Biophys. Acta 1235 (1995) 161–168.
[12] L. Béven, M. Le Hénaff, C. Fontenelle, H. Wróblewski, Curr. Microbiol. 33 (1996) 317–322.
[13] M. Le Hénaff, C. Fontenelle, Arch. Microbiol. 173 (2000) 339–345.

[14] C. Brenner, H. Wróblewski, M. Le Hénaff, L. Montagnier, A. Blanchard, Infect. Immun. 65 (1997) 4322–4329.
[15] C. Chevalier, C. Saillard, J.M. Bové, J. Bacteriol. 172 (1990) 6090–6097.
[16] X. Foissac, J.M. Bové, C. Saillard, Curr. Microbiol. 35 (1997) 240–243.
[17] L. Béven, H. Wróblewski, Res. Microbiol. 148 (1997) 163–175.
[18] L. Béven, D. Duval, S. Rebuffat, B. Bodo, H. Wróblewski, Biochim. Biophys. Acta 1372 (1998) 78–90.
[19] L. Béven, O. Helluin, G. Molle, H. Duclohier, H. Wróblewski, Biochim. Biophys. Acta 1421 (1999) 53–63.
[20] H. Wróblewski, S. Nyström, A. Blanchard, Å. Wieslander, J. Bacteriol. 171 (1989) 5039–5047.
[21] P.K. Smith, R.I. Krohn, G.T. Hermanson, A.K. Mallia, F.H. Gartner, M.D. Provenzano, E.K. Fujimuto, N.M. Goeke, D.C. Klenk, Anal. Biochem. 150 (1985) 76–85.
[22] C. Combet, C. Blanchet, C. Geourjon, G. Deleage, Trends Biochem. Sci. 3 (2000) 147–150.
[23] J.P. Hennessey, W.C. Johnson Jr., Biochemistry 20 (1987) 1085–1094.
[24] D. Blaudez, T. Buffeteau, J.C. Cornut, B. Desbat, N. Escafre, M. Pézolet, J.M. Turlet, Thin Solid Films 242 (1994) 146–150.
[25] D. Blaudez, J.M. Turlet, J. Dufourcq, D. Bard, T. Buffeteau, B. Desbat, J. Chem. Soc., Faraday Trans. 92 (1996) 525–530.
[26] S. Castano, B. Desbat, M. Laguerre, J. Dufourcq, Biochim. Biophys. Acta 1416 (1999) 176–194.
[27] S. Castano, B. Desbat, J. Dufourcq, Biochim. Biophys. Acta 1463 (2000) 65–80.
[28] D.W. Berreman, J. Opt. Soc. Am. 62 (1972) 502–510.
[29] R.H.A. Azzam, N.M. Bashara, Ellipsometry and Polarized Light, North Holland, Amsterdam, 1986, pp. 340–358, Chapter 4.
[30] T. Buffeteau, E. Le Calvez, S. Castano, B. Desbat, D. Blaudez, J. Dufourcq, J. Phys. Chem. B 104 (2000) 4537–4544.
[31] A. Bondon, P. Berthault, I. Segalas, B. Perly, H. Wróblewski, Biochim. Biophys. Acta 1235 (1995) 169–177.
[32] T. Miyazawa, in: G.D. Fasman (Ed.), Poly-α-Amino Acids, vol. 1, Marcel Dekker, New York, 1967, pp. 69–101.
[33] P.I. Haris, D. Chapman, TIBS 17 (1992) 328–333.
[34] W.K. Surewicz, H.H. Mantsch, D. Chapman, Biochemistry 32 (1993) 389–394.
[35] E. Goormaghtigh, V. Cabiaux, J.M. Ruysschaert, in: H.J. Hilderson, G.B. Ralston (Eds.), Subcellular Biochemistry: Physicochemical Methods in the Study of Biomembranes, vol. 23, Plenum, New York, 1994, pp. 363–403.
[36] E. Goormaghtigh, V. Cabiaux, J.M. Ruysschaert, in: H.J. Hilderson, G.B. Ralston (Eds.), Subcellular Biochemistry: Physicochemical Methods in the Study of Biomembranes, vol. 23, Plenum, New York, 1994, pp. 405–450.
[37] I. Cornut, B. Desbat, J.M. Turlet, J. Dufourcq, Biophys. J. 70 (1996) 305–312.
[38] P.F. Smith, in: J. Maniloff, R.N. McElhaney, L.R. Finch, J.B. Baseman (Eds.), Mycoplasmas: Molecular Biology and Pathogenesis, ASM Press, Washington, DC, 1992, pp. 79–91.
[39] H. Vogel, F. Jähnig, V. Hoffman, J. Stümpel, Biochim. Biophys. Acta 733 (1983) 201–209.
[40] S. Frey, L.K. Tamm, Biophys J. 60 (1991) 922–930.
[41] D. Blaudez, F. Boucher, T. Buffeteau, B. Desbat, M. Grandbois, C. Salesse, Appl. Spectrosc. 53 (1999) 1299–1304.
[42] D. Ducharme, J.J. Max, C. Salesse, R.M. Leblanc, J. Phys. Chem. 94 (1990) 1925–1932.
[43] T. Buffeteau, D. Blaudez, E. Péré, B. Desbat, J. Phys. Chem. B 103 (1999) 5020–5027.
[44] T.B. Clark, R.F. Whitcomb, J.G. Tully, C. Mouches, C. Saillard, J.M. Bové, H. Wróblewski, P. Carle, D.L. Rose, B. Henegar, D.L. Williamson, Int. J. Syst. Bacteriol. 35 (1985) 296–308.